Nigerian Journal of Physics (NJP)
ISSN online: 3027-0936
ISSN print: 1595-0611
DOI: https://doi.org/10.62292/njp.v35(s).2026.658
Volume 35(S), 2026

# Surface Morphology and Elemental Composition of Vernonia amygdalina-Sensitized Ternary Chalcogenide Thin Films: A Comparative SEM/EDS Study of CdZnS, ZnSnS, ZnCdSe, CuZnS and CuZnSnS

*[1,2]Godswill Chinonso Nwigwe and [1]Mishark N. Nnabuchi

[1]Department of Industrial Physics, Faculty of Physical Sciences, Enugu State University of Science and Technology (ESUT), Enugu, Nigeria.
[2]Department of Industrial/Medical Physics, David Umahi Federal University of Health Sciences, Uburu, Ebonyi State, Nigeria.

*Corresponding Author's Email: nwigwegodswill@dufuhs.edu.ng

**Keywords**:
Thin films,
Chalcogenides,
SEM,
EDS,
Vernonia amygdalina.

**Submitted**: 20 Jul. 2026

**Accepted**: 3 Aug. 2026

**Published**: 10 Aug. 2026

**ABSTRACT**

The surface morphology and elemental composition of five solution-grown ternary chalcogenide thin films – cadmium zinc sulphide (CdZnS), zinc tin sulphide (ZnSnS), zinc cadmium selenide (ZnCdSe), copper zinc sulphide (CuZnS) and copper zinc tin sulphide (CuZnSnS) – were examined after sensitization with a natural dye extracted from Vernonia amygdalina (bitter leaf), using scanning electron microscopy (SEM) and energy-dispersive spectroscopy (EDS). SEM micrographs of all five dye-sensitized films revealed continuous, grain-covered surfaces consistent with solution-grown chalcogenide films. EDS confirmed the presence of the expected metal and chalcogen constituents in each film – Cd, Zn and S in CdZnS; Zn, Sn and S in ZnSnS; Zn, Cd and Se in ZnCdSe; Cu and Zn and S in CuZnS; and Cu, Zn, Sn and S in CuZnSnS – together with carbon and oxygen attributable to surface adsorbates and dye-related organic residues. The combined oxygen and carbon content varied widely across the series, from 59.4 at.% in CdZnS to 84.4 at.% in ZnCdSe, with ZnSnS, CuZnS and CuZnSnS falling between these extremes, indicating substantially different degrees of dye-related surface coverage on the five host lattices despite identical sensitization conditions. These results confirm successful elemental incorporation of the intended ternary compositions in all five systems and demonstrate that the extent of bitter leaf dye attachment, as judged by surface C and O content, is strongly host-dependent.

## INTRODUCTION

The transition to clean, affordable and sustainable energy systems remains one of the most pressing challenges of contemporary materials research, with thin-film photovoltaic technologies offering a low-material, low-cost alternative to bulk silicon-based solar cells. Among the candidates explored for absorber, buffer and window layers, ternary chalcogenide semiconductors are attractive because their optical band gap, crystal structure, surface chemistry and electrical conductivity can be tuned through compositional variation, deposition conditions and post-deposition surface modification (Minami, 2005; Chen et al., 2010). The solution growth technique (also referred to as chemical bath deposition) is widely used for depositing such films because it is simple, inexpensive, scalable, operates at low temperature and does not require vacuum infrastructure, making it particularly suited to resource-limited research environments (Pramanik et al., 1988; Al-Jawad & Alioy, 2013; Ouafi et al., 2018; Sengupta et al., 2023).

A complementary and increasingly important strategy for improving the visible-light response of semiconductor thin films is sensitization with natural plant-derived dyes. Such dyes are inexpensive, biodegradable, locally available and free of the toxicity and cost concerns associated with many synthetic sensitizers (Wongcharee et al., 2007; O'Regan & Grätzel, 1991). Vernonia amygdalina (bitter leaf), a plant widely available across Nigeria and other parts of sub-Saharan Africa, contains phytochemical pigments and oxygen-bearing functional groups (hydroxyl, carbonyl and carboxyl moieties) capable of anchoring to semiconductor surfaces and

modifying their optical, chemical and electrical response (Wongcharee et al., 2007).

In the present series of investigations, five ternary chalcogenide thin-film systems – cadmium zinc sulphide (CdZnS), zinc tin sulphide (ZnSnS), zinc cadmium selenide (ZnCdSe), copper zinc sulphide (CuZnS) and copper zinc tin sulphide (CuZnSnS) – were deposited on glass substrates by the solution growth technique and divided into as-grown and Vernonia amygdalina dye-sensitized sets. These five systems span both n-type (CdZnS, ZnSnS, ZnCdSe) and p-type (CuZnS, CuZnSnS) conduction, wide-gap to narrow-gap behaviour, and sulphide- and selenide-based chemistries, providing a representative cross-section of low-cost chalcogenide materials relevant to buffer, window and absorber layers in thin-film photovoltaic devices (Chen et al., 2010; Lokhande et al., 1998). Reporting the results as a coordinated series allows the influence of a single, common natural sensitizer to be compared systematically across chemically distinct host lattices.

Scanning electron microscopy (SEM) and energy-dispersive spectroscopy (EDS) provide complementary information on the surface morphology and elemental composition of thin films, and are particularly useful for confirming successful incorporation of the intended ternary stoichiometry and for detecting surface-bound species introduced by post-deposition treatments such as dye sensitization (Emegha et al., 2022; Agbo & Nnabuchi, 2011). This paper reports a comparative SEM/EDS study of dye-sensitized CdZnS, ZnSnS, ZnCdSe, CuZnS and CuZnSnS thin films, with the aim of confirming elemental incorporation across the five systems and evaluating the relative extent of bitter leaf dye attachment on each host lattice. The UV-Visible absorbance and optical band-gap data referred to in Section 3.6 for cross-comparison with the present SEM/EDS results were obtained on the same as-grown and dye-sensitized film sets as part of a companion investigation by the present authors (Nwigwe & Nnabuchi, unpublished data) and are cited here only for context.

## MATERIALS AND METHODS

### Materials

Analytical-grade precursors were used as obtained, with distilled water as solvent for all aqueous solutions. Glass microscope slides served as substrates for all five film systems. Ammonia solution, triethanolamine (TEA) and/or ethylenediaminetetraacetic acid (EDTA) were used as complexing agents and pH adjusters to regulate the rate of free metal-ion release during deposition.

### Substrate Preparation

Glass substrates were degreased by immersion in concentrated hydrochloric acid for 24 h, washed in detergent solution, scrubbed gently with a soft sponge, rinsed repeatedly with distilled water and air-dried. Clean substrates promote uniform nucleation, good adhesion and reproducible film growth.

### Preparation of Vernonia amygdalina Dye Extract

Fresh bitter leaf (Vernonia amygdalina) leaves were washed thoroughly with distilled water to remove surface contaminants. Ten grams of cleaned leaves were placed in 100 mL of distilled water and heated at 80-85 °C for 1 h to extract the natural pigments and phytochemical constituents. The leaves were then removed and the resulting extract was allowed to cool before use as the sensitizing medium.

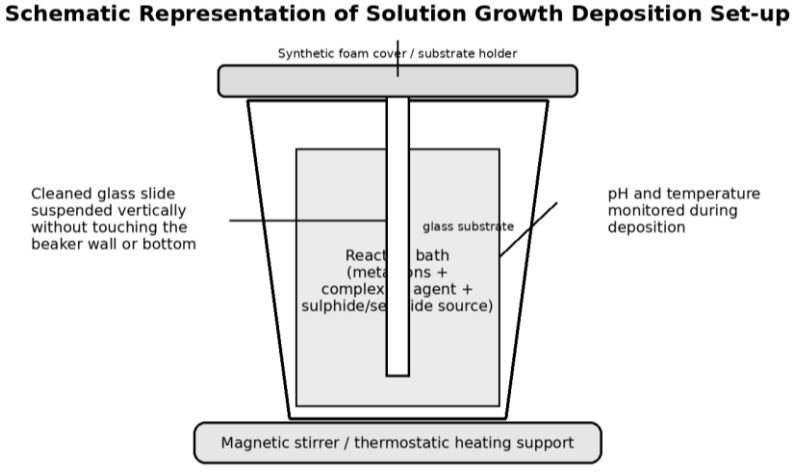


Figure 1: Schematic representation of the solution growth deposition set-up used for all five film systems

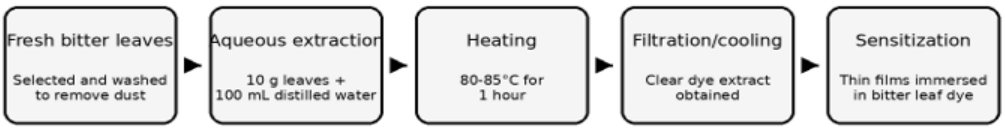


Figure 2: Extraction and application sequence for Vernonia amygdalina (bitter leaf) dye sensitization

**Deposition of the Five Ternary Chalcogenide Thin-Film Systems**

Five ternary chalcogenide thin-film systems were deposited by the solution growth technique under bath conditions optimised for each chemistry. In each case, the cleaned substrates were suspended vertically in the reaction bath for a deposition time of 45 minutes and temperature of $80^0$C, after which they were rinsed with distilled water, dried in air and divided into two sets: an as-grown set retained for characterization, and a dye-sensitized set immersed in the Vernonia amygdalina extract, rinsed lightly and dried at room temperature.

CdZnS films were deposited from cadmium acetate dihydrate [Cd(CH3COO)2·2H2O, 0.02 M], zinc nitrate hexahydrate [Zn(NO3)2·6H2O, 0.02 M] and thioacetamide (CH3CSNH2, 0.03 M) in ammoniacal solution:

$Cd(CH_3COO)_2 + Zn(NO_3)_2 + 2CH_3CSNH_2 + 6OH^- \rightarrow CdS\downarrow + ZnS\downarrow + 4CH_3COO^- + 2NO_3^- + 2NH_3 + 2H_2O$ *(co-deposited as the* $Cd_{1-x}Zn_xS$ *solid solution denoted CdZnS)*

ZnSnS films were deposited from zinc nitrate hexahydrate [Zn(NO3)2·6H2O, 0.02 M], tin(II) chloride (SnCl2, 0.02 M) and thioacetamide (0.03 M):

$Zn(NO_3)_2 + SnCl_2 + 2CH_3CSNH_2 + 6OH^- \rightarrow ZnS\downarrow + SnS\downarrow + 2NO_3^- + 2Cl^- + 2CH_3COO^- + 2NH_3 + 2H_2O$ *(co-deposited as the Zn1-xSnxS solid solution denoted ZnSnS)*

ZnCdSe films were deposited from zinc nitrate hexahydrate [Zn(NO3)2·6H2O, 0.02 M], cadmium acetate dihydrate [Cd(CH3COO)2·2H2O, 0.02 M] and selenourea as the selenium precursor [$SeC(NH_2)_2$, 0.02 M]:

$Zn(NO_3)_2 + Cd(CH_3COO)_2 + 2SeC(NH_2)_2 + 4OH^- \rightarrow ZnSe\downarrow + CdSe\downarrow + 2NO_3^- + 2CH_3COO^- + 2NH_2CN + 4H_2O$ *(co-deposited as the* $Zn_{1-x}Cd_xSe$ *solid solution denoted ZnCdSe;* $NH_2CN$ *= cyanamide, the alkaline hydrolysis by-product of selenourea)*

CuZnS films were deposited from copper sulphate ($CuSO_4$, 0.02 M), zinc nitrate hexahydrate [$Zn(NO_3)_2·6H_2O$, 0.02 M] and thioacetamide (0.03 M) under alkaline conditions:

$CuSO_4 + Zn(NO_3)_2 + 2CH_3CSNH_2 + 6OH^- \rightarrow CuS\downarrow + ZnS\downarrow + SO_4^{2-} + 2NO_3^- + 2CH_3COO^- + 2NH_3 + 2H_2O$ *(co-deposited as the* $Cu_{1-x}Zn_xS$ *solid solution denoted CuZnS)*

CuZnSnS films were deposited from copper sulphate (CuSO4, 0.02 M), zinc nitrate hexahydrate [$Zn(NO_3)_2·6H_2O$, 0.02 M], tin(II) chloride ($SnCl_2$, 0.02 M) and thioacetamide (0.03 M), giving the charge-balanced kesterite-type composition $Cu_2ZnSnS_4$:

$2CuSO_4 + Zn(NO_3)_2 + SnCl_2 + 4CH_3CSNH_2 + 12OH^- \rightarrow Cu_2ZnSnS_4\downarrow + 2SO_4^{2-} + 2NO_3^- + 2Cl^- + 4CH_3COO^- + 4NH_3 + 4H_2O$

**Morphological and Compositional Characterization**

Surface morphology of the dye-sensitized films was examined by scanning electron microscopy (SEM) at 500× magnification, using an accelerating voltage of 10.00 kV and working distances of approximately 10-13 mm across the five specimens (as recorded in the SEM image metadata), while energy-dispersive spectroscopy (EDS) provided the elemental composition (atomic and weight percentages and net counts) of each film, including carbon and oxygen signals associated with surface adsorbates and dye-related organic residues.

## RESULTS AND DISCUSSION

Table 1 summarizes the combined carbon and oxygen content (an indicator of dye-related surface coverage) and the principal metal/chalcogen constituents detected by EDS for each dye-sensitized film. The five materials are discussed individually in subsequent sections, followed by a cross-comparison.

**Table 1: Summary of EDS-detected constituents and combined carbon + oxygen content (surface dye indicator) for the five dye-sensitized ternary chalcogenide thin films**

| Material | Expected constituents (EDS-confirmed) | C (at.%) | O (at.%) | C+O (at.%) |
|---|---|---|---|---|
| CdZnS | Cd, Zn, S | 4.1 | 55.3 | 59.4 |
| ZnSnS | Zn, Sn, S | 6.9 | 68.1 | 75.0 |
| ZnCdSe | Zn, Cd, Se | 11.9 | 72.5 | 84.4 |
| CuZnS | Cu, Zn, S | 8.5 | 72.8 | 81.3 |
| CuZnSnS | Cu, Zn, Sn, S | 9.5 | 53.4 | 62.9 |

**Cadmium Zinc Sulphide (CdZnS)**

SEM imaging of the dye-sensitized CdZnS film revealed a granular, surface-covering morphology consistent with solution-grown chalcogenide films, while EDS confirmed the presence of cadmium, zinc and sulphur together with carbon and oxygen, the latter two attributed to surface adsorbates and dye-related organic residues. The elemental composition is summarized in Table 2.

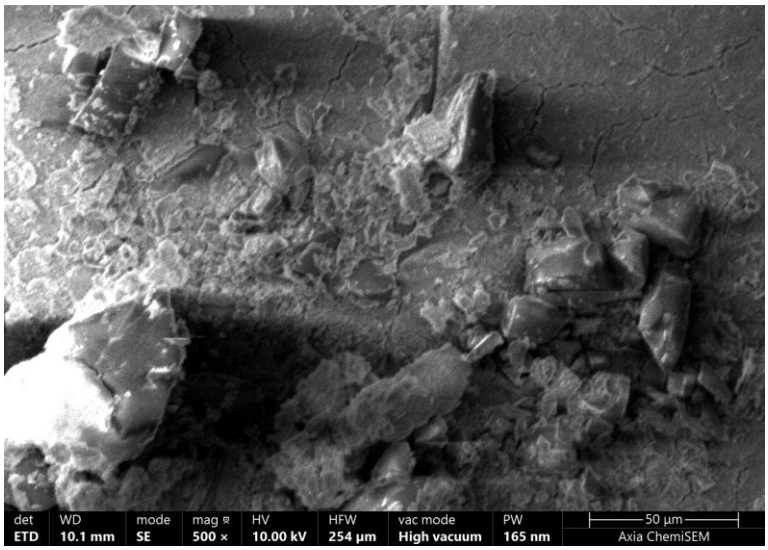


Figure 3: SEM micrograph of dye-sensitized CdZnS thin film at 500× magnification

**Table 2: SEM/EDS elemental composition of dye-sensitized CdZnS thin film**

| Element | Line | At. % | Wt. % | Net counts |
|---|---|---|---|---|
| C | K | 4.1 | 1.4 | 249 |
| O | K | 55.3 | 25.5 | 4,269 |
| S | K | 14.7 | 13.5 | 3,487 |
| Zn | L | 17.9 | 33.8 | 5,918 |
| Cd | L | 8.0 | 25.8 | 2,073 |

The EDS spectrum confirms the presence of the expected Cd, Zn and S constituents of CdZnS, while the relatively high oxygen and carbon content reflects surface oxidation and the adsorption of bitter-leaf-derived organic species onto the film surface, consistent with successful sensitization.

**Zinc Tin Sulphide (ZnSnS)**

SEM imaging of the dye-sensitized ZnSnS film showed a continuous, grain-covered surface, while EDS (Table 3) confirmed the presence of zinc, tin and sulphur together with carbon and oxygen attributed to surface adsorbates and dye-related organic residues.

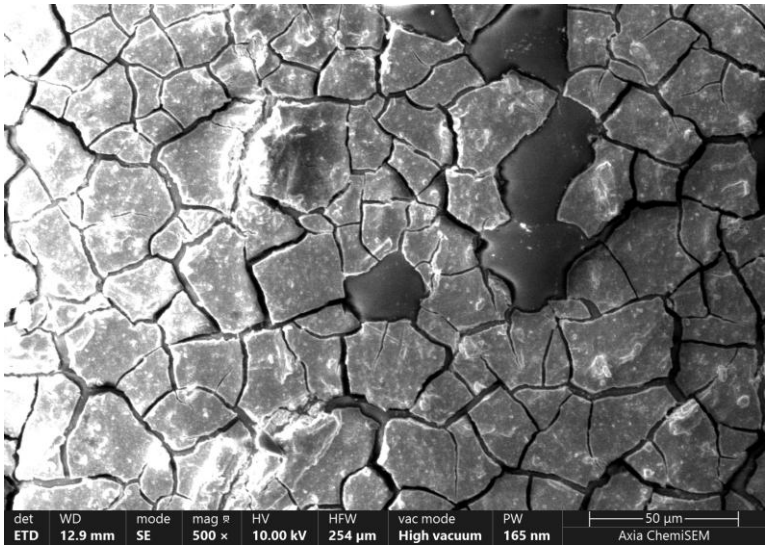


Figure 4: SEM micrograph of dye-sensitized ZnSnS thin film at 500× magnification

**Table 3: SEM/EDS elemental composition of dye-sensitized ZnSnS thin film**

| Element | Line | At. % | Wt. % | Net counts |
|---|---|---|---|---|
| C | K | 6.9 | 2.1 | 18,352 |
| O | K | 68.1 | 27.9 | 88,683 |
| S | K | 1.1 | 0.9 | 4,777 |
| Zn | L | 2.5 | 4.1 | 10,788 |
| Sn | L | 21.4 | 65.0 | 92,082 |

The EDS result confirms the presence of the expected Zn, Sn and S constituents of ZnSnS, while the high oxygen and carbon content is consistent with substantial surface coverage by dye-related organic species, supporting the strong increase in visible absorbance observed for this film by UV-Visible spectroscopy. The measured metal/chalcogen ratio (Zn:Sn ≈ 1:8.6, S = 1.1 at.%) deviates markedly from the nominal 1:1:1 ternary stoichiometry; given the very high combined C+O content (75.0 at.%) recorded on the same spectrum, this is most plausibly explained by strong attenuation of the shallow S Kα and Zn Lα signals by a thick dye-derived organic overlayer, which would depress the apparent chalcogen and Zn signal relative to the more penetrating Sn Lα line, rather than by genuine bulk non-stoichiometry; low-accelerating-voltage operation and substrate interference cannot presently be excluded and are noted as limitations.

**Zinc Cadmium Selenide (ZnCdSe)**

SEM imaging of the dye-sensitized ZnCdSe film showed a continuous surface morphology, while EDS (Table 4) confirmed the presence of zinc, selenium and cadmium together with the highest combined carbon and oxygen content observed in this series, attributable to surface adsorbates and dye-related organic residues.

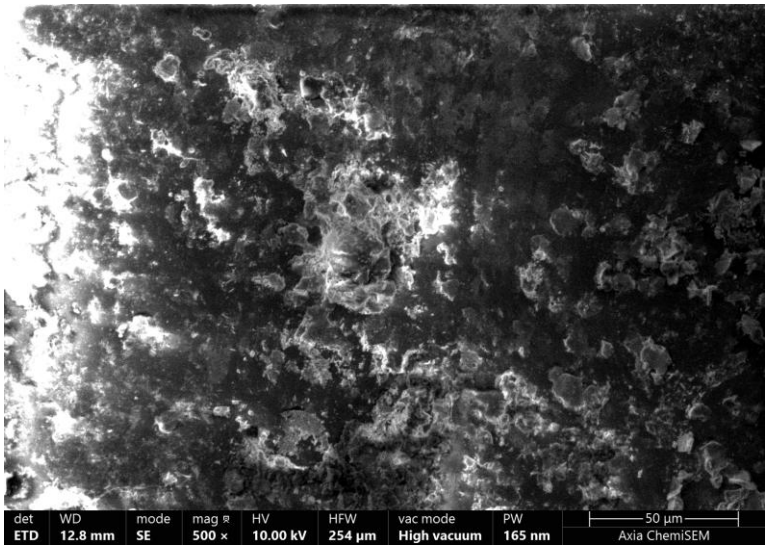


Figure 5: SEM micrograph of dye-sensitized ZnCdSe thin film at 500× magnification

**Table 4: SEM/EDS elemental composition of dye-sensitized ZnCdSe thin film**

| Element | Line | At. % | Wt. % | Net counts |
|---|---|---|---|---|
| C | K | 11.9 | 6.0 | 17,897 |
| O | K | 72.5 | 48.6 | 166,139 |
| Zn | L | 13.3 | 36.5 | 84,505 |
| Se | L | 1.3 | 4.3 | 8,527 |
| Cd | L | 1.0 | 4.6 | 4,448 |

The EDS result confirms the presence of the expected Zn, Cd and Se constituents of ZnCdSe, while the high oxygen and carbon levels (84.4 at.% combined, the highest of the series) reflect extensive dye-related surface coverage, consistent with the strong increase in absorbance observed by UV-Visible spectroscopy for this film. As with ZnSnS, the very low Se (1.3 at.%) and Cd (1.0 at.%) signals relative to Zn are consistent with strong attenuation by the exceptionally thick organic overlayer implied by the 84.4 at.% combined C+O content, rather than genuine bulk non-stoichiometry; this interpretation should be verified by repeat measurements at higher accelerating voltage or after mild surface cleaning to reduce overlayer attenuation.

**Copper Zinc Sulphide (CuZnS)**

SEM imaging of the dye-sensitized CuZnS film showed an absorber-related surface morphology with reasonable compactness, while EDS (Table 5) confirmed the presence of copper, zinc and sulphur together with carbon and oxygen attributable to surface adsorbates and dye-related organic residues.

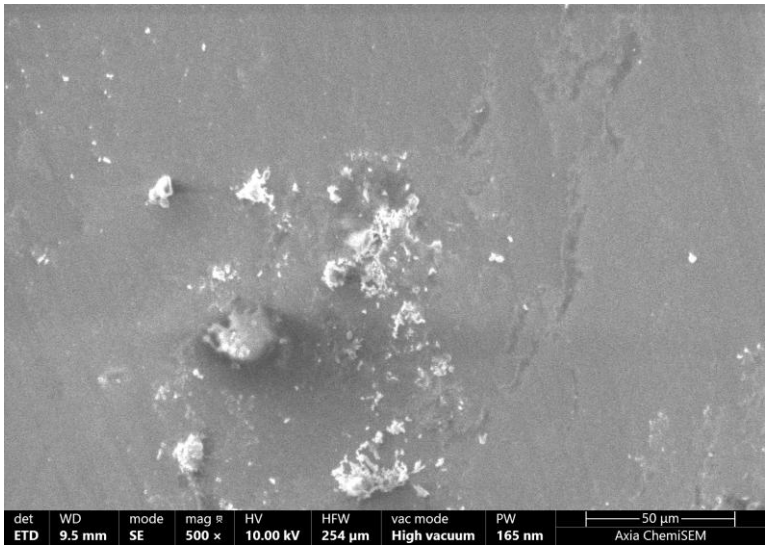


Figure 6: SEM micrograph of dye-sensitized CuZnS thin film at 500× magnification

**Table 5: SEM/EDS elemental composition of dye-sensitized CuZnS thin film**

| Element | Line | At. % | Wt. % | Net counts |
|---|---|---|---|---|
| C | K | 8.5 | 4.3 | 3,550 |
| O | K | 72.8 | 48.5 | 55,748 |
| S | K | 2.0 | 2.7 | 2,595 |
| Cu | L | 13.3 | 35.3 | 18,944 |
| Zn | L | 3.4 | 9.2 | 4,448 |

The EDS result confirms the presence of the expected Cu, Zn and S constituents of CuZnS, while the high oxygen and carbon content (81.3 at.% combined) reflects substantial surface coverage by dye-related organic species, consistent with the increase in absorbance observed by UV-Visible spectroscopy for this film. The comparatively low S signal (2.0 at.%) relative to Cu and Zn again mirrors the pattern seen for ZnSnS and ZnCdSe and is attributed to attenuation of the shallow S Kα line by the thick dye-derived overlayer rather than to a genuinely sulphur-deficient film.

**Copper Zinc Tin Sulphide (CuZnSnS)**

SEM imaging of the dye-sensitized CuZnSnS film showed an absorber-related surface morphology, while EDS (Table 6) confirmed the presence of copper, zinc, tin and sulphur together with carbon and oxygen attributable to surface adsorbates and dye-related organic residues.

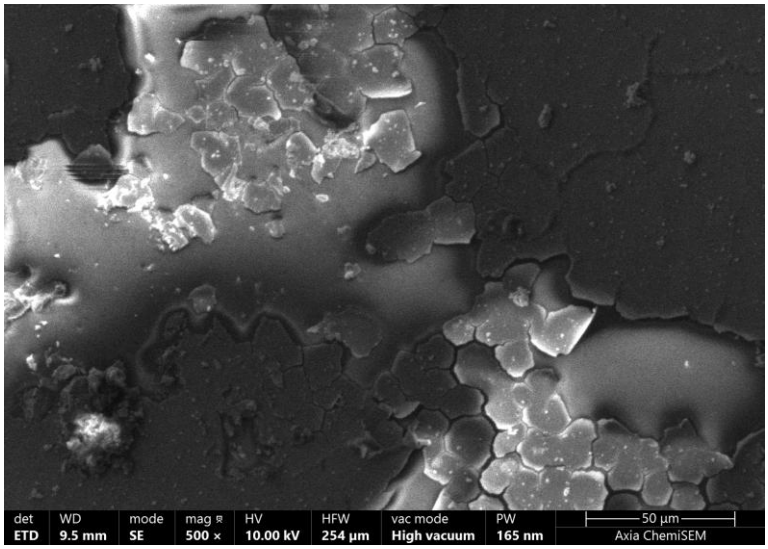


Figure 7: SEM micrograph of dye-sensitized CuZnSnS thin film at 500× magnification

**Table 6: SEM/EDS elemental composition of dye-sensitized CuZnSnS thin film**

| Element | Line | At. % | Wt. % | Net counts |
|---|---|---|---|---|
| C | K | 9.5 | 3.9 | 3,069 |
| O | K | 53.4 | 29.0 | 36,507 |
| S | K | 13.3 | 14.4 | 19,332 |
| Cu | L | 15.3 | 33.1 | 26,649 |
| Zn | L | 8.0 | 17.8 | 13,131 |
| Sn | L | 0.5 | 1.8 | 678 |

The EDS result confirms the presence of all four expected metal constituents (Cu, Zn, Sn) together with S, supporting successful deposition of the intended CuZnSnS system, while the carbon and oxygen content (62.9 at.% combined, the second lowest of the series) reflects a more moderate degree of surface dye coverage relative to ZnCdSe and CuZnS. The low Sn signal (0.5 at.%) relative to Cu, Zn and S is consistent with modest organic-overlayer attenuation of the Sn Lα line and/or a genuine Sn-poor surface region of the kesterite-type film, and warrants confirmation by depth-resolved or cross-sectional EDS in future work.

**Cross-Comparison of Morphological and Compositional Trends**

EDS confirmed the expected metal and chalcogen constituents in all five ternary systems, demonstrating that the intended compositions were successfully realized by the solution growth technique across chemically distinct precursor chemistries; however, several films (notably ZnSnS, ZnCdSe, CuZnS and, to a lesser extent, CuZnSnS) showed pronounced deviations from the nominal 1:1:1 (or 2:1:1:4 for CuZnSnS) metal/chalcogen ratios, with chalcogen and minor-metal signals systematically suppressed relative to the dominant metal. Because these deviations track closely with the combined C+O content across the series (Table 1), the most consistent explanation is attenuation of the shallow, low-energy chalcogen and minor-metal X-ray lines by a thick, dye-derived organic overlayer on the film surface, rather than genuine bulk non-stoichiometry; contributions from the fixed 500× imaging condition and possible substrate interference at low signal depths cannot be ruled out with the present data and should be addressed in follow-up measurements at higher accelerating voltage and after controlled overlayer removal. The combined carbon and oxygen content – used here as a proxy for the extent of bitter-leaf-derived surface coverage – ranged from 59.4 at.% (CdZnS) to 84.4 at.% (ZnCdSe), with ZnCdSe and CuZnS showing the highest values (84.4 and 81.3 at.%, respectively) and CdZnS and CuZnSnS the lowest (59.4 and 62.9 at.%, respectively). Interestingly, the two films with the highest surface C+O content (ZnCdSe and CuZnS) were also among those showing the largest increases in UV-Visible absorbance and the largest optical band-gap blue shifts after sensitization, suggesting a possible correlation between the extent of dye adsorption detected by EDS and the magnitude of the optical response to sensitization. CdZnS, which showed the lowest combined C+O content, was also the only film exhibiting a band-gap red shift rather than a blue shift,

consistent with a more limited but still influential dye-surface interaction.

## CONCLUSION

A comparative SEM/EDS study of five Vernonia amygdalina dye-sensitized ternary chalcogenide thin films – CdZnS, ZnSnS, ZnCdSe, CuZnS and CuZnSnS – has confirmed continuous, grain-covered surface morphologies and the presence of the expected metal and chalcogen constituents in every system, alongside carbon and oxygen signals attributable to dye-related surface residues. The combined carbon and oxygen content varied from 59.4 to 84.4 at.% across the series, with ZnCdSe and CuZnS showing the most extensive apparent dye coverage and CdZnS the least. These results confirm successful elemental incorporation of the intended ternary compositions in all five systems and indicate that the degree of bitter leaf dye attachment, and its associated optical consequences, are strongly host-dependent. Several films also showed pronounced deviations of the measured chalcogen and minor-metal atomic percentages from nominal stoichiometry, most plausibly arising from attenuation of shallow X-ray signals by the dye-derived surface overlayer; future work will include depth-resolved EDS and measurements at higher accelerating voltage, together with controlled overlayer removal, to confirm this interpretation and refine the bulk stoichiometry estimates.

## ACKNOWLEDGEMENTS

The authors gratefully acknowledge the Department of Industrial Physics, Enugu State University of Science and Technology (ESUT), for providing laboratory facilities used in this work.

## REFERENCES

Agbo, P. E., & Nnabuchi, M. N. (2011). Core-shell TiO2/ZnO thin film: Preparation, characterization and effect of temperature on some selected properties. Chalcogenide Letters, 8(4), 273-282. URL: https://chalcogen.ro/273_Agbo.pdf

Al-Jawad, S. M. H., & Alioy, F. H. (2013). Kinetics of growth and structural characterization of Cd1-xZnxS thin films synthesized by CBD method. Engineering and Technology Journal, 31(4B), 505-519. https://doi.org/10.30684/etj.31.4B.9

Chen, S., Gong, X. G., Walsh, A., & Wei, S. H. (2010). Defect physics of the kesterite thin-film solar cell absorber Cu2ZnSnS4. Applied Physics Letters, 96(2), 021902. https://doi.org/10.1063/1.3275796

Emegha, J. O., Ukhurebor, K. E., Aigbe, U. O., Damisa, J., & Babalola, A. V. (2022). Synthesis and characterization of copper zinc iron sulphide (CZFS) thin films. Heliyon, 8(8), e10331. https://doi.org/10.1016/j.heliyon.2022.e10331

Lokhande, C. D., Patil, P. S., Tributsch, H., & Ennaoui, A. (1998). ZnSe thin films by chemical bath deposition method. Solar Energy Materials and Solar Cells, 55(4), 379-393. https://doi.org/10.1016/S0927-0248(98)00112-3

Minami, T. (2005). Transparent conducting oxide semiconductors for transparent electrodes. Semiconductor Science and Technology, 20(4), S35-S44. https://doi.org/10.1088/0268-1242/20/4/004

O'Regan, B., & Grätzel, M. (1991). A low-cost, high-efficiency solar cell based on dye-sensitized colloidal TiO2 films. Nature, 353, 737-740. https://doi.org/10.1038/353737a0

Ouafi, M., Jaber, B., Atourki, L., Zayyoun, N., Ihlal, A., Mzerd, A., & Laânab, L. (2018). In situ low-temperature chemical bath deposition of CdS thin films without thickness limitation: Structural and optical properties. International Journal of Photoenergy, 2018, Article 4549154. https://doi.org/10.1155/2018/4549154

Pramanik, P., Akhter, M. A., & Basu, P. K. (1988). Chemical bath deposition of manganese sulphide thin films. Thin Solid Films, 158, 271-276. https://doi.org/10.1016/0040-6090(88)90030-2

Sengupta, S., Aggarwal, R., & Raula, M. (2023). A review on chemical bath deposition of metal chalcogenide thin films for heterojunction solar cells. Journal of Materials Research, 38, 142-153. https://doi.org/10.1557/s43578-022-00539-9

Wongcharee, K., Meeyoo, V., & Chavadej, S. (2007). Dye-sensitized solar cell using natural dyes extracted from rosella and blue pea flowers. Solar Energy Materials and Solar Cells, 91(7), 566-571. https://doi.org/10.1016/j.solmat.2006.11.005